FREQUENCY COMPARISON (H_MASER 1400816) - (BNM-SYRTE-FO2) from MJD 53199 to MJD 53224

The primary frequency standard BNM-SYRTE-FO2 was compared to the hydrogen maser (1400816) of the laboratory, from MJD 53199 to MJD 53224.

The mean fractional frequency differences measured between the hydrogen Maser and fountain FO2 during this period is given in table 1:

Period (MJD)	Y(H_Maser 1400816) – Y(FO2) (1)	u_B (2)	u_A (3)	$u_{link\ /\ maser}$ (4)
53199 – 53224	+3378,5	**6,5**	**0,57**	**1,92**

Table 1: Results of the comparison in 1 x 10^{-16} unit.

Figure 1 collects the measurements of fractional frequency differences during the 12th July to 7 August period. The measurements are corrected for the systematic frequency shifts listed below.

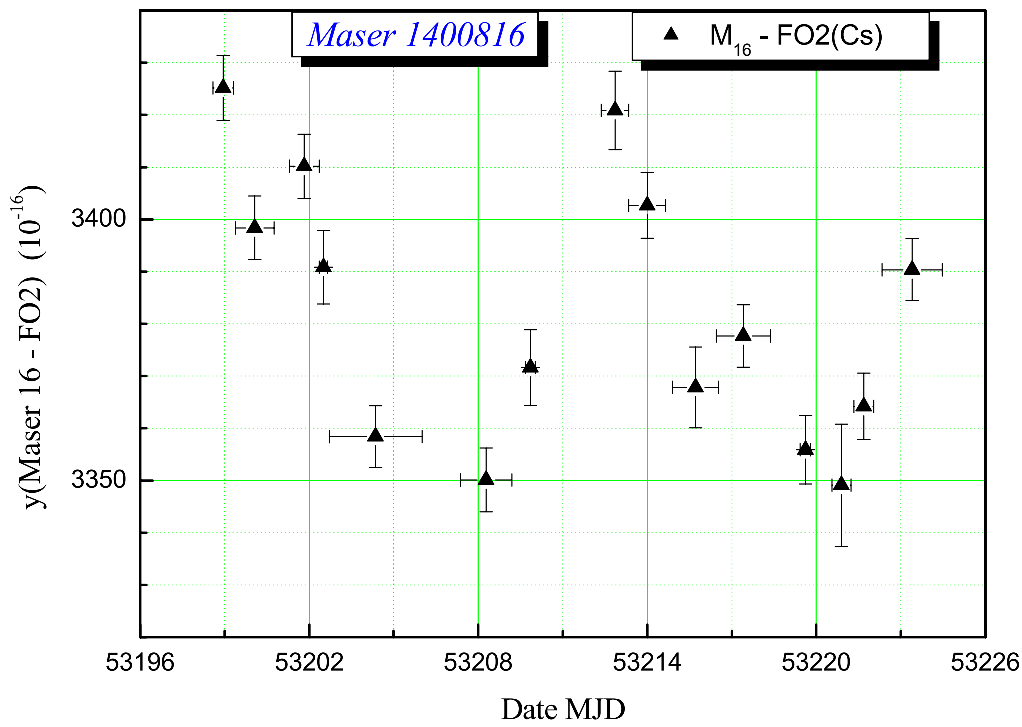

Figure 1: fractional frequency differences between H_Maser1400816 & FO2 from MJD 53199 to MJD 53224

Table of measurements is given bellow (table 2).

Start UTC dates unit MJD	Start Local dates unit H:M	Duration H :M	Mean fractional frequency difference $y_{Maser} - y_{FO2}$	type A uncertainties σ_{Stat}	$\sigma_{Collision}$
53198,58542	12/07/2004 16:03	17:29	3,42517E-13	1,53E-16	1,89E-16
53199,39167	13/07/2004 11:24	32:38	3,39839E-13	1,17E-16	1,42E-16
53201,30417	15/07/2004 09:18	25:13	3,41015E-13	1,34E-16	1,65E-16
53202,36181	16/07/2004 10:41	07:07	3,39082E-13	2,56E-16	3,05E-16
53202,72361	16/07/2004 19:22	78:42	3,35841E-13	7,27E-17	9,04E-17
53207,37153	21/07/2004 10:55	43:51	3,35013E-13	1,26E-16	1,57E-16
53209,67639	23/07/2004 18:14	08:28	3,37163E-13	2,92E-16	3,32E-16
53212,37014	26/07/2004 10:53	23:14	3,42087E-13	3,1E-16	3,69E-16
53213,34514	27/07/2004 10:17	31:17	3,40268E-13	1,62E-16	1,98E-16
53214,72222	28/07/2004 19:20	38:58	3,36784E-13	1,34E-16	5E-16
53216,44236	30/07/2004 12:37	46:13	3,37769E-13	9,7E-17	1,19E-16
53219,42847	02/08/2004 12:17	08:46	3,35588E-13	2,03E-16	2,36E-16
53220,55069	03/08/2004 15:13	16:19	3,34909E-13	1,75E-16	1E-15
53221,33333	04/08/2004 10:00	16:45	3,36421E-13	1,71E-16	2,05E-16
53222,32778	05/08/2004 09:52	51:25	3,39037E-13	9,6E-17	1,17E-16

Table 2: Measurements H_Maser1400816 - FO2 from MJD 53199 to 53224

Start UTC dates unit MJD	Stop UTC dates unit MJD	Duration & Measurement Rate	Mean frequency difference normalized $y_{Maser} - y_{FO2}$ **(1)**	type A uncertainty σ_{Stat} & $\sigma_{Collision}$	Uncertainty due to the dead times $\sigma_{deadTime}$ **(4)**
53198,58542	53224,47014	Total duration : 25,88472 j Total measurements 18,594 j Measurement Rate : 71,8356%	Standard Mean $\bar{y}$ = **3382,2** x **10^{-16}** Weighted Mean **(5)**: $\bar{y}$ = **3379,9 x 10^{-16}** Linear fit regression **(6)**: $\bar{y}$ = **3379,6 x 10^{-16}** Mean from Phase differences **(7)**: $\bar{y}$ = **3378,5 x 10^{-16}**	σ_A = 0,**564 10^{-16} (3)** Linear fit regression σ_A = 0,**567 10^{-16} (6)** From Phase differences σ_A = (0,**57) 10^{-16}**	$\sigma_{deadTime}$ = **(1,92) 10^{-16}**

Table 3: Statistics of measurements

(1) Fractional frequency difference obtained after systematic relative frequency shifts correction:

$$y_{Maser - FOM} = \frac{\delta(\nu)_{Zeeman2}}{\nu_0} + \frac{\delta(\nu)_{BlackBody}}{\nu_0} + \frac{\delta(\nu)_{Collision + CavityPulling}}{\nu_0} + \frac{\delta(\nu)_{redshift}}{\nu_0} - \frac{f_{mesure}}{\nu_0}$$

with $\nu_0 := 0.9192631770 \quad 10^{10}$. The fractional mean frequency is calculated by four ways as mentioned in table 3 in order to have comparison between statistical computation such as standard mean, weighted mean, with a linear fit and with phase differences.

(2) Systematic uncertainty $\sigma_B = u_B$ in witch statistical effect of cold collisions and cavity pulling is removed (see **Annexe 1**)

$$\sigma_B = \left(\sigma_{Zeeman2}{}^2 + \sigma_{BlackBody}{}^2 + \sigma_{Collision_{Syst}}{}^2 + \sigma_{Microwave\_Spectrum}{}^2 + \sigma_{Microwave\_Leakage}{}^2 + \sigma_{Ramsey\_Rabi}{}^2 + \sigma_{Recoil}{}^2 + \sigma_{second\_Doppler}{}^2 + \sigma_{Background\_collsions}{}^2 + \sigma_{Redshift}{}^2 \right)^{(1/2)}$$

(3) Statistical uncertainty $\sigma_A = u_A$, in which is taken into account the statistical uncertainty on each measurement σ_{Stat_i} and statistical effect on the cold collisions and Cavity Pulling measurement $\sigma_{Collision_i}$ (see **Annexe 4** Linear Regression on the frequency measurements & **Annexe 5**) : $\sigma_A = \sqrt{\dfrac{1}{\displaystyle\sum_{i=1}^{n} \dfrac{1}{\sigma_{Stat_i}{}^2 + \sigma_{Collision_i}{}^2}}}$

(4) Uncertainty due to the link between H_Maser and the fountain FO2 $u_{link\_Maser} = \sqrt{\sigma_{link\_Lab}{}^2 + \sigma_{dead\_time}{}^2}$ where $\sigma_{link\_Lab} = 0.1\ 10^{-15}$ and σ_{dead_time} is the uncertainty due to the dead times during measurements (see **Annexe 3**)

(5) Weighted Mean by statistical uncertainty on each measurement

$$y_j := \frac{\displaystyle\sum_{i=1}^{n_j} \frac{y_i}{\sigma_{Ai}{}^2}}{\displaystyle\sum_{i=1}^{n_j} \frac{1}{\sigma_{Ai}{}^2}}$$

where

$$\sigma_{A_i} = \frac{1}{\sqrt{\dfrac{1}{\sigma_{Stat_i}{}^2 + \sigma_{Col_i}{}^2}}}$$

(6) Mean frequency obtained by a linear fit by weighted least squares with statistical uncertainty on each measurement (see **Annexe 4**).

(7) Mean frequency obtained by phase differences that is the retained result (see **Annexe 5**).

ANNEXE 1

Uncertainties of systematic effects in the FO2 fountain

Systematic effects taken into account are the quadratic Zeeman, the Black Body, the cold collision and cavity pulling corresponding to the systematic part (see annexe 2), the microwave spectral purity and the microwave leakage, the Ramsey Rabi pulling, the recoil, the 2nd Doppler and the background collisions. Each of these effects are affected by an uncertainty. The uncertainty of the red shift effect is also included in the systematic uncertainty budget and gives

$$\sigma_B = \left(\sigma_{Zeeman2}{}^2 + \sigma_{BlackBody}{}^2 + \sigma_{Collision_{Syst}}{}^2 + \sigma_{Microwave\_Spectrum\_Leakage}{}^2 + \sigma_{first\_Doppler}{}^2 + \sigma_{Ramsey\_Rabi}{}^2 + \sigma_{Recoil}{}^2 + \sigma_{second\_Doppler}{}^2 + \sigma_{Background\_collisions}{}^2 + \sigma_{Redshift}{}^2 \right)^{(1/2)}$$

Here are mentioned the uncertainties of the different effects (see **Annexe 2** and **[ref, 1]**):

Quadratic Zeeman effect	:	$\sigma_{Zeeman2} := 0.3\ 10^{-16}$	(continuously measured)
Black Body effect	:	$\sigma_{BlackBody} := 0.25\ 10^{-15}$	(calculated)
Systematic Collisional effect	:	$\sigma_{Collision_{Syst}} := 0.3409\ 10^{-15}$	(continuously measured)
Microwave Spectrum purity & Leakage effect	:	$\sigma_{Microwave\_Spectrum\_Leakage} = 0.33\ 10^{-15}$	(measured)
First order Doppler effect	:	$\sigma_{first\_Doppler} < 0.3\ 10^{-15}$	(calculated and measured)
Rabi-Ramsey effect	:	$\sigma_{Ramsey\_Rabi} < 0.10\ 10^{-15}$	(calculated)
Recoil effect (see **[ref, 3]**)	:	$\sigma_{Recoil} < 0.14\ 10^{-15}$	(calculated)
Second order Doppler effect	:	$\sigma_{second\_Doppler} := 0.8\ 10^{-17}$	(calculated)
Background effect	:	$\sigma_{Background\_collisions} := 0.10\ 10^{-15}$	(evaluated)
Red shift effect	:	$\sigma_{Redshift} := 0.1\ 10^{-15}$	(calculated)

For the whole July period it gives

$$=> \boxed{\sigma_B = 0.652\ 10^{-15}}$$

ANNEXE 2

1 - Measurement of the collisional frequency shift and the cavity pulling

Collisional shift takes into account the effect of the collisions between cold Caesium atoms and the effect of "Cavity Pulling" whose influence also depends on the number of atom. This effect is measured in a differential way during each integration and its determination thus depends on the duration of the measurement and on the stability of the clock, thus the uncertainty on the determination of the collisional shift is mainly of statistical nature. To the statistical uncertainty we add a type B uncertainty of 1% of frequency shift resulting from the imperfection of the adiabatic passage method (see the article **[ref. 4]**).

Figure 2 visualizes the relative frequency shift due to the effect of the collisions and "Cavity Pulling" of the atomic fountain FO2 taken in low density, between the MJD 53199 and 53224 with the statistical uncertainty of each measurement, $\sigma_{Collision(i)}$.

Figure 3 shows the Allan deviation of a differential measurement using high and half atom density fountain configurations during MJD 53202 (from MJD 53202,72361 to MJD 53206,00278), in order to correct of the cold collisional shift for this period. FO2 was operated alternatively (every 50 clock cycles) at low atomic density (red circle) and high density (black square) against the cryogenic oscillator weakly phase locked on the H_Maser. The measured density ratio between low and high densities is 0,5006±0,0002. The frequency difference between both densities is used to determine the collisional coefficient which is used to correct each data point. The blue triangle points represent the Allan deviation of the frequency difference between low and high densities when the points are corrected. The Allan deviation varies as $\tau^{-1/2}$and reaches 10^{-16} after 3 days of integration (78H42mn).

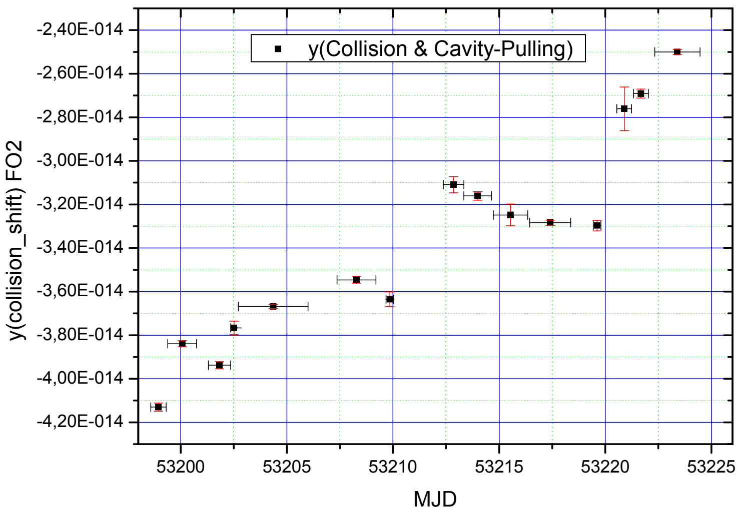

Figure 2: Fractional frequency shift due to cold collisions and Cavity Pulling from MJD 53199 to MJD 53224

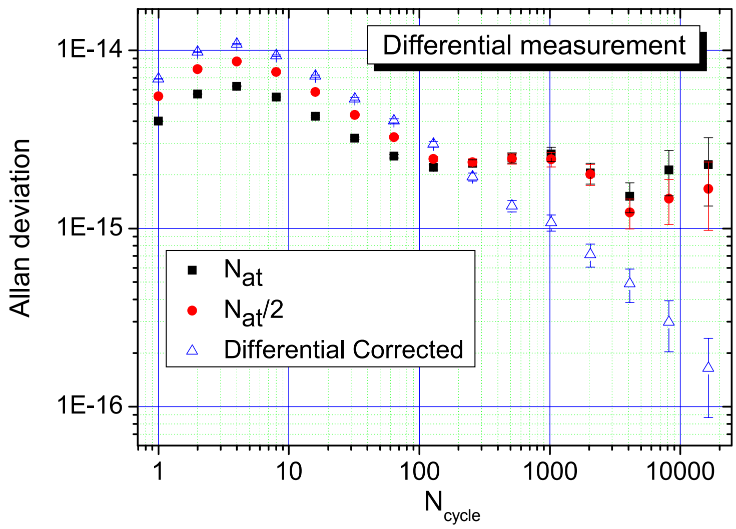

Figure 3: Allan deviation of measurements of the shift frequency in high and low atom density and their differences during MJD 53202,72361 to MJD 53206,00278

The weighted mean $y_{Collision_{moy}} = \dfrac{\sum_{i=1}^{n} \dfrac{y_{Collision_i}}{\sigma_{Collision_i}^2}}{\sum_{i=1}^{n} \dfrac{1}{\sigma_{Collision_i}^2}}$ of collisionnal shift gives for the July period $y_{Collision_{moy}} := -0.3409 \ 10^{-13}$

The systematic effect of these shifts is evaluated by the 1% part of the mean frequency collisional shift during July:

$$\sigma_{Collision_{Syst}} = \frac{1}{100} \left| y_{Collision_{moy}} \right| = \sigma_{Collision_{Syst}} := 0.3409 \ 10^{-15}$$

This value is taking into account in the systematic uncertainty evaluation σ_B (see annexe 1).

2 - Measurement of the 2nd order Zeeman frequency shift

Every 15 min the frequency of the central fringe of the field linearly dependant transition $|F=3, m_F=1\rangle \longrightarrow |F=4, m_F=1\rangle$ is measured. This frequency is directly proportional to the field as $\delta(\nu_{11})=K_{Z1}B$ with K_{Z1} = 7,0084 Hz.nT^{-1} (see **[ref. 5]** vol. 1 p37 table 1.1.7(a)). In the fountain, the transition $|F=3, m_F=0\rangle \longrightarrow |F=4, m_F=0\rangle$ is shifted by quadratic Zeeman effect and depend on squared magnetic field as $\delta(\nu_{00})=K_{Z2}B^2$ with K_{Z1} = 42,745 mHz.µT^{-2} (see **[ref. 5]** vol. 1 p37 table 1.1.7(a)). Knowing K_{Z1} and measuring δ(ν11) allow good estimation of Zeeman quadratic shift as $\delta(\nu_{00}) = K_{Z1}\left(\dfrac{\delta(\nu_{11})}{K_{Z1}}\right)^2$. The relative quadratic Zeeman frequency shift is calculated by $\dfrac{\delta(\nu_{00})}{\nu_0} = 427{,}45\times10^{-6}\left(\dfrac{\delta(\nu_{11})}{700{,}84}\right)^2$ with $\delta(\nu_{11})$ in Hz unit and ν_0 = 9192631770 Hz. And the uncertainty is evaluated by $\dfrac{\Delta(\delta(\nu_{00}))}{\nu_0} = 427{,}45\times10^{-6}\times\dfrac{2\times\overline{B}\times\Delta(B)}{\nu_0}$ with B in mG. Figure 4 displays the tracking of the central fringe during MJD 53198 to MJD 53226. This shows the good stability of the magnetic field in the interrogation zone. The frequency variation is taken as in an interval of standard deviation ±0,094Hz. When taking the standard deviation of variation of the magnetic field $\Delta(B)$ over the whole measurement period as the field uncertainty, we find 13 pT. The corresponding uncertainty of the correction of the second order Zeeman effect is 0,3x10^{-16}.

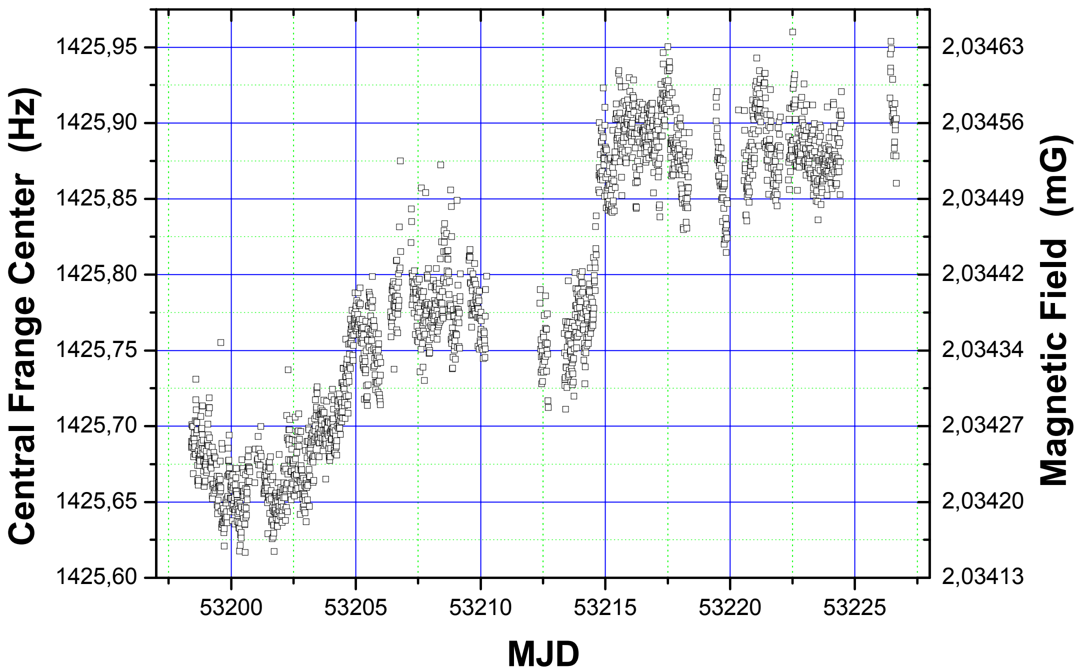

Figure 4: tracking of the central fringe from MJD 53198 to MJD 53226

3 - Measurement of the Blackbody Radiation shift

An ensemble of 3 platinum thermistors monitors the temperature and its gradient inside the vacuum chamber. The average temperature is ~25,5°C with a gradient smaller than 1 K along the atom trajectory. The correction is

$$\left(\frac{\delta(\nu)}{\nu_0}\right)_{Blackbody} = -\frac{0.0001573\left(\frac{T}{300}+0.9105000000\right)^4}{\nu_0} = -0.168281\ 10^{-13} \pm 0.25\ 10^{-15}$$

4 - Effect of the Microwave Spectrum effect and leakage effect

The clock frequency is measured as a function of the microwave power. Every 50 cycles the atom interrogation is alternated between 4 configurations of π/2, low density and high density, and 3π/2, low density and high density. It allows extrapolating and removing the variation of the collision shift in the comparison between π/2 and 3π/2 pulses. We find

$$\frac{\delta(\nu)_{Microwave\_Spectrum\_Leakage}}{\nu_0} = -0.44\ 10^{-15} \pm 0.33\ 10^{-15}$$

5 - Measurement of the residual 1st order Doppler effect

We determined the frequency shifts caused by asymmetry of the coupling coefficients of the two microwave feedthroughs and the error on the launching direction by coupling the interrogation signal either “from the right” or “from the left” or symmetrically into the cavity. The measured shift is

$$\left(\frac{\delta(\nu)}{\nu_0}\right)_{first\_Doppler} = 0.45\ 10^{-14} \pm 0.11\ 10^{-15}$$

In FO2 fountain we feed the cavity symmetrically at 1% level both in phase and in amplitude. This shift is thus reduced by a factor of 100 and became negligible. The quadratic dependence of the phase becomes dominant. A worse case estimate based on **[ref. 6]** gives fractional frequency shift of 3 x 10^{-16} which we take as uncertainty due to the residual 1st order Doppler effect.

6 – Rabi and Ramsey effect and Majorana transitions effect

An imbalance between the residual populations and coherences of $m_F < 0$ and $m_F > 0$ states can lead to a shift of the clock frequency estimated to few 10^{-18} for a population imbalance of 10^{-3} that we observe in FO2 (see **[ref. 7]** and **[ref. 8]**).

7 – Microwave recoil effect

The shift due to the microwave photon recoil was investigated in **[ref. 3]**. It is smaller than 1,4 x 10^{-16} .

8 – Gravitational red-shift and 2nd order Doppler shift

The relativistic effect is evaluated as: $\frac{\delta(\nu)_{redshift}}{\nu_0} = 0.625\ 10^{-14}$ with an uncertainty $\sigma_{Redshift} = \pm\ 0.1\ 10^{-15}$

The 2nd order Doppler shift is less than 0,08 x 10^{-16} .

9 – Background collisions effect

The vacuum pressure inside the fountains is typically a few 10^{-8} Pa. Based on early measurements of pressure shift (see **[ref. 5]**) the frequency shift due to collisions with the background gas is < 10^{-16}.

ANNEXE 3

Uncertainty due to the dead time during the measurements

A statement of the distribution of the missed periods of measurements by FO2 is represented in figure 5,

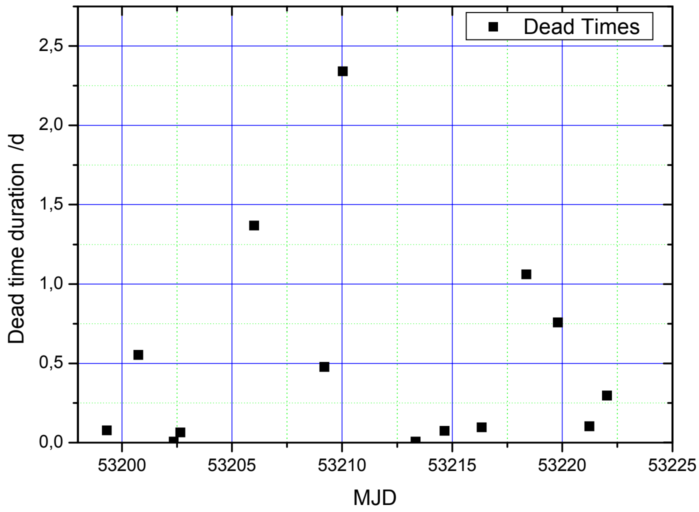

Figure 5 : Dead Times on measurements of H_ Maser1400816 –FO2 over the period from MJD 53199 to 53224

For the period of the MJD 53199 until the MJD 53224, the variations of phase between hydrogen Maser 1400805 and the hydrogen Maser 1400816 were sampled every 100s. After removing a linear fit from the phase variations to carry out the calculation of standard deviation in the temporal field, we evaluated the uncertainty associated with the H_Maser according to time (by step of 100s). One obtains the phase variations between H_Maser 1400805 and the H_Maser 1400816. They are plotted on figure 6.

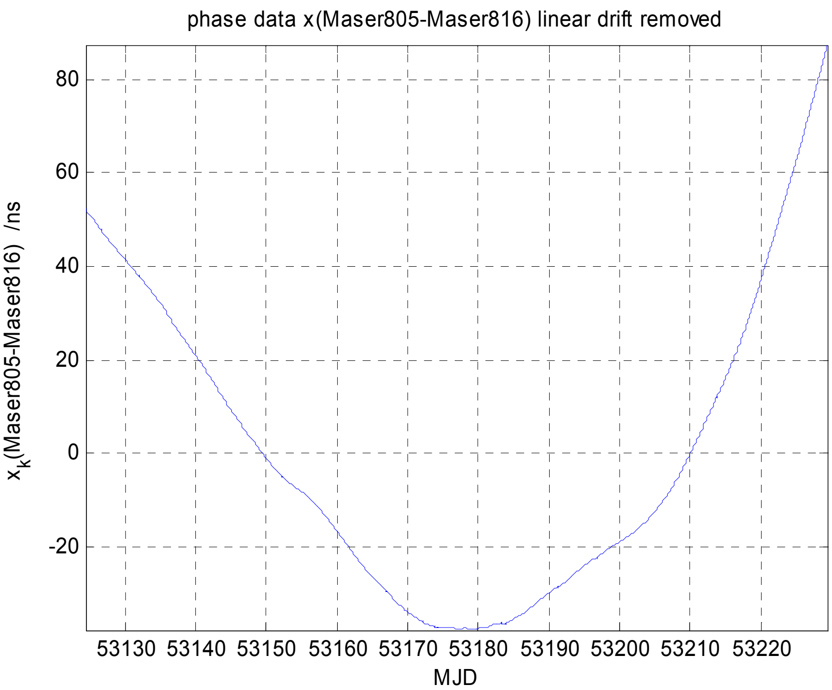

figure 6 : x(H805-H816) MJD 53124 to MJD 53229 linear fit removed

Frequency stability analyzes were performed using the overlapping Allan deviation on frequency data and represented for May to August in figure 7 and similarly time stability analyzes with a time deviation were computed and represented for May to August in figure 8 .

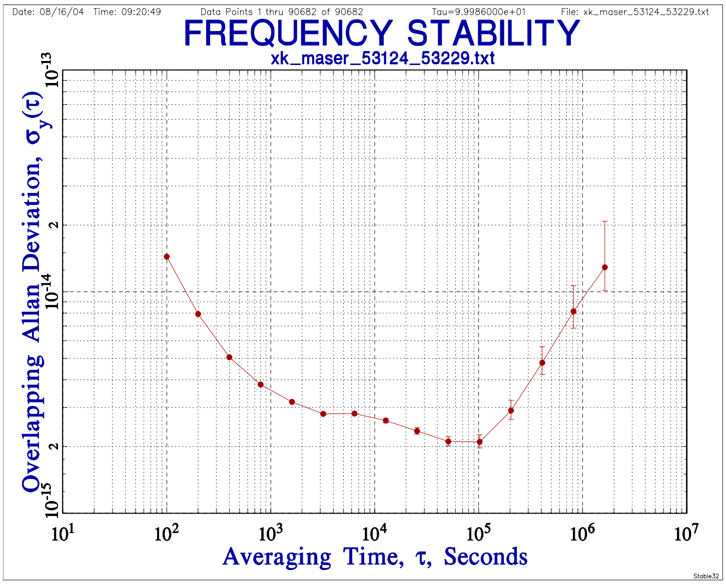

figure 7 : frequency stability analyzes x(HMaser805 - HMaser816) from MJD 53124 to MJD 53229

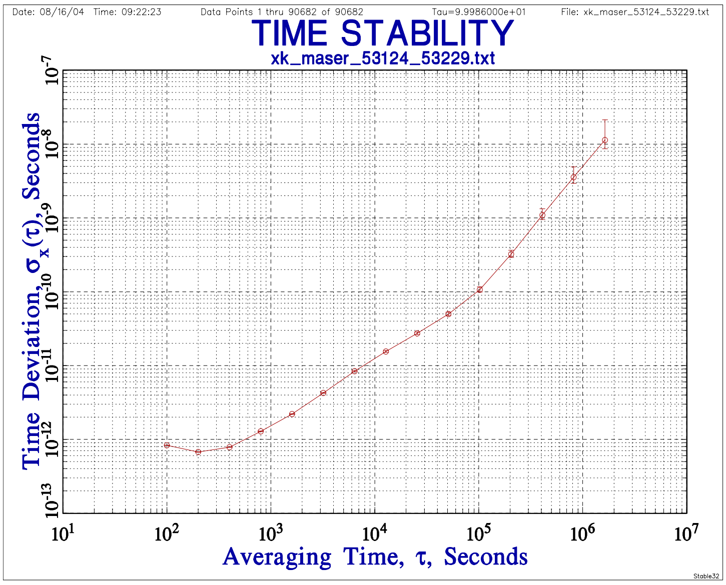

figure 8 : time stability analyzes from x(HMaser805 - HMaser816) from MJD 53124 to MJD 53229

Table 4 provides the standard deviations of the phase fluctuations of the hydrogen Maser 1400805 with respect to the hydrogen Maser 1400816 associated to each dead time according to their duration for the period May to August 2004. The quadratic sum gives

$$\sum_{i=1}^{15} \sigma_{x_i}(\tau)^2 = 0.1349455047 \quad 10^{-18}$$

During the July 2004 period of FO2 measurements 25,88 days or $T = 0.223643980799953 \quad 10^{7}$ seconds. One thus finds the standard deviation of the fluctuations of frequency due to the dead times in measurements by the ratio

$$\sigma_{deadTime} = \frac{\sqrt{\sum_{i=1}^{15} \sigma_{x_i}(\tau)^2}}{T} = 0.1643 \quad 10^{-15}$$

With taking $\sigma_{link\_Maser} = \sqrt{\sigma_{link\_lab}^{2} + \sigma_{deadTime}^{2}}$ that gives $\boxed{\sigma_{link\_Maser} = 0.1923 \quad 10^{-15}}$

End Date of each measurement (MJD)	Dead Time Duration HH : M	second	σ_x
13/07/2004 09:32	01:52	6720	8,86580E-12
14/07/2004 20:02	13:16	47760,00001	4,68560E-11
16/07/2004 10:31	00:10	600	1,03180E-12
16/07/2004 17:48	01:34	5639,99999	7,55720E-12
20/07/2004 02:04	32:51	118259,99999	1,31290E-10
23/07/2004 06:46	11:28	41279,99999	4,11510E-11
24/07/2004 02:42	56:11	202260,00001	3,16330E-10
27/07/2004 10:07	00:10	600	1,03180E-12
28/07/2004 17:34	01:46	6359,99998	8,39660E-12
30/07/2004 10:18	02:19	8339,99999	1,06960E-11
01/08/2004 10:50	25:27	91620,00001	9,26300E-11
02/08/2004 21:03	18:10	65400	6,30610E-11
04/08/2004 07:32	02:28	8879,99999	1,12570E-11
05/08/2004 02:45	07:07	25620	2,73570E-11
07/08/2004 13:17			

Table 4: Statement of the dead times of H_Maser 1400816 - FO2 measurements between MJD 53199 and MJD 53224

ANNEXE 4

Linear Regression on the frequency measurements on period MJD 53199-53224

One calculates the linear regression line by the algorithm of weighted least squares by statistical uncertainty of each frequency differences measurements:

$$y_k = a_1 + a_2\, t$$

Figure 9 gives the representation of frequency measurements and the linear fit resulting from weighted least squares by inverse of squares statistical uncertainty $1/\sigma_{Ai}^{\ 2}$.

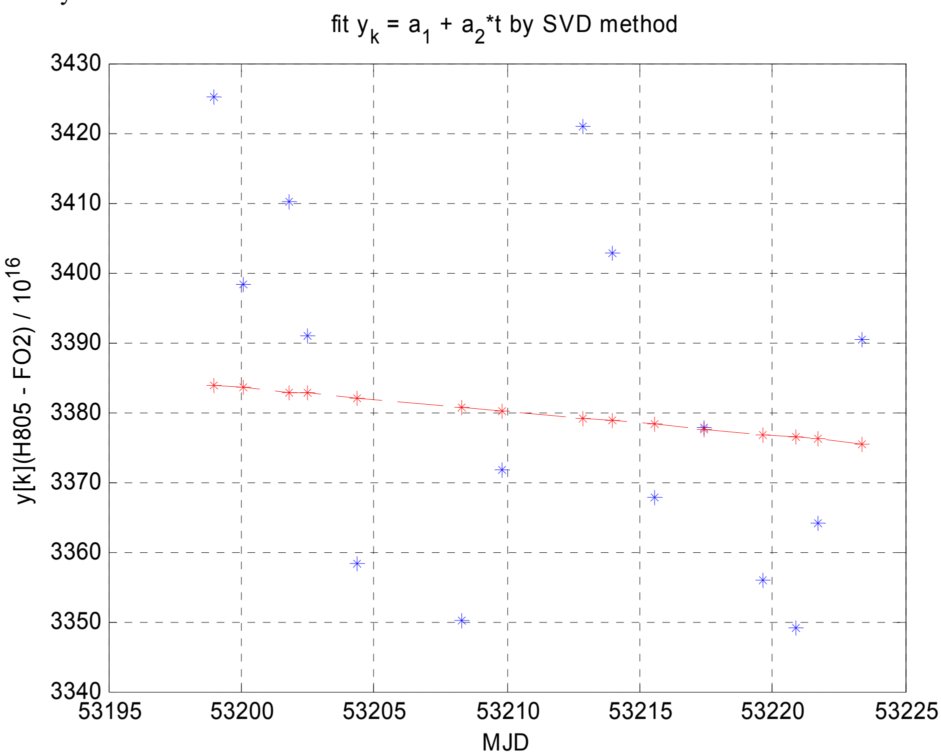

Figure 9: linear regression on the frequency y(HMaser-FO2) between MJD 53199 and 53224 weighted by uncertainty : $1/\sigma_{Ai}^{\ 2}$

Summary of statistical terms :

Coefficient a1 = 2,16491829530574e-012 sigma(a1) of yk FO2 =3,52752113172836e-013
Coefficient a2 = -3,43339774582651e-017 sigma(a2) of yk FO2 =6,62939420840918e-018

Covariance Matrix:

1,24434053347901e-025	-2,33853278611918e-030
-2,33853278611918e-030	4,39488675704891e-035

Mean date of measurements	=	53211,174305
Frequency mean by linear fit y_FO2	=	3,37967036190051e-013
Uncertainty propagation at t_mean uc_y_FO2	=	5,67501511681957e-017

Degree of Freedom DEF	=	13
Mean Square Error = Chi2/DEF	=	115,87424957166
Birge ratio Rb = (chi2/DEF)^1/2	=	10,7644902142024
Limit of Birge ratio Rb = 1+sqrt(2/DEF)	=	1,39223227027637
Probability of a sample y(HMaser-FO2) being superior of Chi2|DEF	=	9,112666073927453e-315
SSR Sum Square of Residues	=	8,26820976619011e-029
RMS Root Mean Square of Residues	=	9,09296968332684e-015
Allan Variance	=	2,968347642857136e-030
Allan Deviation	=	1,722889329834373e-015
Allan Deviation at T with assumption of White Frequency Noise	=	4,307223324585933e-016
T durée totale + tau0	=	2385535,7951995 (seconds)
tau0 (mean time between measurements)	=	149096 (seconds)

Mean Frequency computed by phase differences

On figure 10 is represented the evolution of the differences in fractional frequency y(t). At each period of integration is evaluated a frequency $\tilde{y}_k$ corresponding to the interval $t_{k+1} - t_k$. The relation binding the variations of phase and the instantaneous frequency deviations is given by

$$y_k = \frac{x_{k+1} - x_k}{t_{k+1} - t_k} \qquad (1)$$

$$y(t) = \frac{\nu_{HMaser} - \nu_{FO2}}{\nu_0}$$

$\nu_0 = 9{,}192631770$ GHz

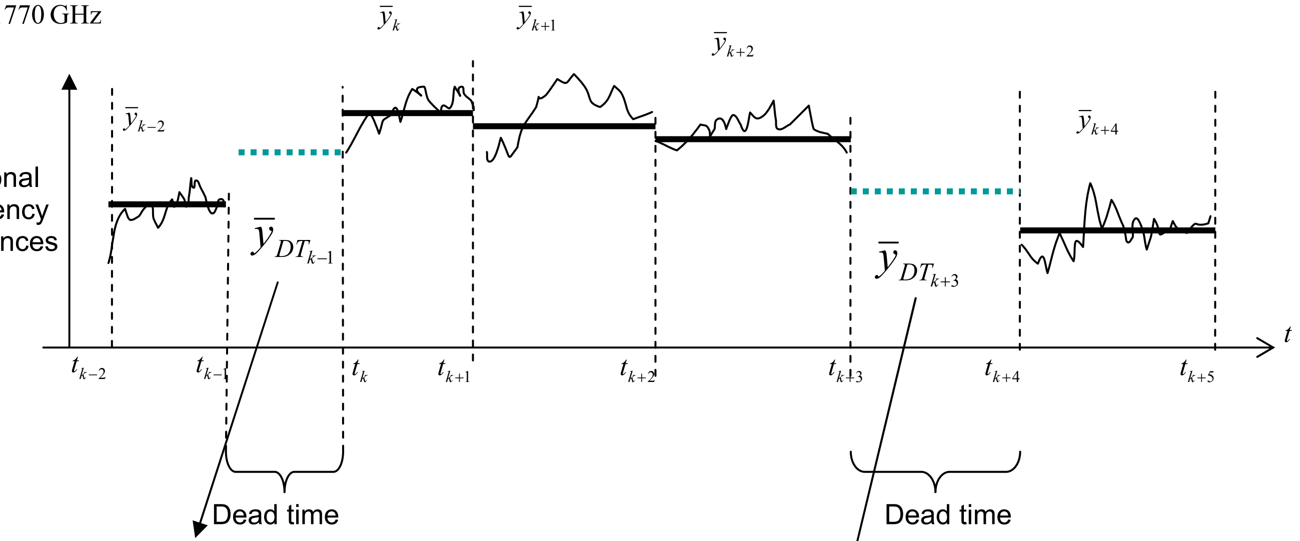

$$\bar{y}_{DT_{k-1}} = \frac{x_k - x_{k-1}}{t_k - t_{k-1}} = \frac{\bar{y}_k + \bar{y}_{k-2}}{2} \qquad \bar{y}_{DT_{k+3}} = \frac{x_{k+4} - x_{k+3}}{t_{k+4} - t_{k+3}} = \frac{\bar{y}_{k+4} + \bar{y}_{k+3}}{2}$$

figure 10 : contribution of frequency measurements on the mean frequency calculated

By using equation (1) we have $x_{k+1} - x_k = (t_{k+1} - t_k)\, y_k$

and for addition of consecutive phase differences we find $\sum_{k=1}^{N} (x_{k+1} - x_k) = x_{N+1} - x_1 = \sum_{k=1}^{N} (t_{k+1} - t_k)\, y_k$

During dead time we evaluated the mean frequency by interpolating the mean frequency between two intervals of integrations noted:

$$y_{DT_{m-1}} = \frac{1}{2} y_m + \frac{1}{2} y_{m-1} \qquad (2)$$

The contributions of N duty intervals with the frequency measurements y_k and M idle intervals with the mean frequency extrapolating between two intervals of integration y_{DT} give the summation

$$\left(\sum_{k=1}^{N} (t_{k+1} - t_k)\, y_k \right) + \left(\sum_{m=1}^{M} (t_{m+1} - t_m)\, y_{DT_m} \right) = x_{fin} - x_{deb} \qquad (3)$$

$$\boxed{y_{moy} = \frac{x_{fin} - x_{deb}}{86400\ MJD_{fin} - 86400\ MJD_{deb}}} \qquad (4)$$

Where $x_{fin} - x_{deb}$ represent the phase variation between the whole periods of integration.

SYRTE 61, avenue de l'Observatoire 75014 Paris - France tél 33 (0)1 40 51 22 04 fax 33 (0)1 40 51 22 91 e-mail direction.syrte@obspm.fr
Unité de recherche du CNRS 8630 site syrte.obspm.fr

The evaluation of statistical uncertainty on each phase differences data extracted from fractional frequency differences, is given as we have in presence of white frequency noise in each period of measurement, by the expression

$$\sigma_x(\tau_i)^2 = \sigma_y(\tau_i)^2\ \tau_i^2$$

For the whole period T of measurement that gives in frequency instability

$$\sigma_y(\tau) = \frac{\sqrt{\sum_{i=1}^{N} \sigma_y(\tau_i)^2\ \tau_i^2}}{T}$$

With N =15, from 12th July to 7th August and $T = 0.223643980799953\ \ 10^7$ seconds it gives

$$\sigma_y(\tau) = \frac{\sqrt{\sum_{i=1}^{15} \sigma_y(\tau_i)^2\ \tau_i^2}}{T} = 0.575\ \ 10^{-16}$$

$$\boxed{\sigma_A = 0.575\ \ 10^{-16}}$$

The evaluation of the mean frequency between two intervals of integrations during the period from MJD 53199 to MJD 53224 is given by equation (2) and calculated for frequency fluctuation difference measurements. Figure 11 shows the frequency differences between H_Maser 1400816 and FO2 (blue plus) and the mean frequency during dead times (magenta stars).

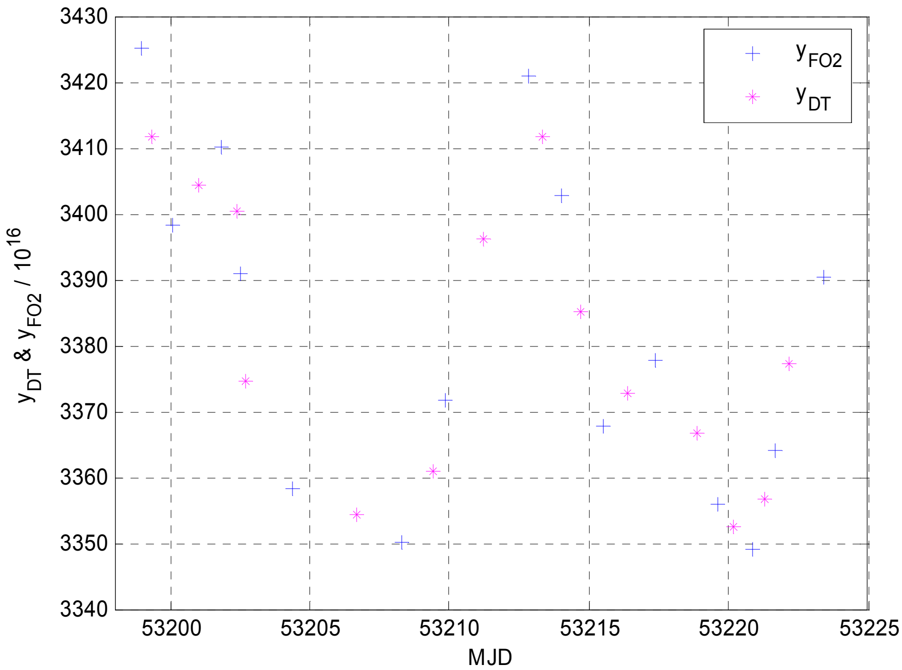

figure 11 : frequency differences H_Maser1400816 and FO2 from MJD 53199 up to MJD 53224

From equation (3) we find the phase difference over the whole period of integration

$$x_{fin} - x_{deb} = 75.558842\ \ \mu s$$

This value is replaced in equation (4) above for computation of y_{moy} during this period. We find

$$\boxed{y_{moy} = 0.33785\ \ 10^{-12}}$$

REFERENCES

[ref. 1] - C. Vian, P. Rosenbusch, H. Marion, S. Bize, L. Cacciapuoti, S. Zhang, M. Abgrall, D. Chambon, I. Maksimovic, P. Laurent, G. Santarelli, A. Clairon of Obs. Paris, SYRTE, A. Luiten, M. Tobar, Univ. W. of Australia School of Physics, C. Salomon of LKB, "BNM-SYRTE Fountains: Recent Results", to be published in **Proceedings CPEM 2004**.

[ref. 2] - F. Pereira Do Santos, H. Marion, M. Abgrall, S. Zhang, Y. Sortais, S. Bize, I. Maksimovic, D. Calonico, J. Grünert, C. Mandache, C. Vian, P. Rosenbusch, P. Lemonde, G. Santarelli, Ph. Laurent and A. Clairon of BNM-SYRTE, C. Salomon of LKB, "Rb and Cs Laser Cooled Clocks: Testing the Stability of Fundamental Constants". **Proceedings IEEE 2003, EFTF Tampa May 2003, p 55-67.**

[ref. 3] - P. Wolf of BNM SYRTE, C.J. Bordé of LPL, "Recoil effects in microwave Ramsey spectroscopy", arxiv: **quant-ph/0403194**.

[ref. 4] - F. Pereira Do Santos, H. Marion, S. Bize, Y. Left, With Bugle, and C. Solomon "Controlling the Cold Collision Shift in High Precision Atomic Interferometry" of, **Phys, Rev, Lett, 89,233004 (2002)**.

[ref. 5] - J. Vanier, C. Audouin, « The Quantum Physics of Atomic Frequency Standards », **Adam Hilger, Bristol & Philadelphia (1989)**.

[ref. 6] - R. Schröder, U. Hübner and D. Griebsch, "Design and Realization of the Microwava Cavity in PTB Caesium Atomic Clock CSF1" **IEEE Trans. Instrum. Meas., vol. 49, p.383, 2002**.

[ref. 7] - L. Cutler *et al*, "Frequency pulling by hyperfine σ - transitions in cesium atomic frequency standards, **J. Appl. Phys. Vol. 69, pp. 2780, 1991**.

[ref. 8] - A. Bauch, R. Schröder "Frequency shift in Caesium Atomic Clock due to Majorana transitions", **Ann. Physics, vol. 2, pp. 421, 1993**.